



UNIVERSITY OF LEEDS

This is a repository copy of *Modelling contraction flows of bi-disperse polymer blends using the RoliePoly and Rolie-Double-Poly equations*.

White Rose Research Online URL for this paper:  
<http://eprints.whiterose.ac.uk/150557/>

Version: Accepted Version

---

**Article:**

Azahar, AA, Harlen, OG [orcid.org/0000-0002-4593-3547](https://orcid.org/0000-0002-4593-3547) and Walkley, MA [orcid.org/0000-0003-2541-4173](https://orcid.org/0000-0003-2541-4173) (2019) Modelling contraction flows of bi-disperse polymer blends using the RoliePoly and Rolie-Double-Poly equations. *Korea Australia Rheology Journal*, 31 (4). pp. 203-209. ISSN 1226-119X

<https://doi.org/10.1007/s13367-019-0021-6>

---

© 2019 The Korean Society of Rheology and Springer. This is an author produced version of a paper published in *Korea-Australia Rheology Journal*. Uploaded in accordance with the publisher's self-archiving policy.

**Reuse**

Items deposited in White Rose Research Online are protected by copyright, with all rights reserved unless indicated otherwise. They may be downloaded and/or printed for private study, or other acts as permitted by national copyright laws. The publisher or other rights holders may allow further reproduction and re-use of the full text version. This is indicated by the licence information on the White Rose Research Online record for the item.

**Takedown**

If you consider content in White Rose Research Online to be in breach of UK law, please notify us by emailing [eprints@whiterose.ac.uk](mailto:eprints@whiterose.ac.uk) including the URL of the record and the reason for the withdrawal request.



[eprints@whiterose.ac.uk](mailto:eprints@whiterose.ac.uk)  
<https://eprints.whiterose.ac.uk/>

# Modelling contraction flows of bi-disperse polymer blends using the RoliePoly and Rolie-Double-Poly equations

Adila A Azahar<sup>1,2</sup>, Oliver G Harlen<sup>3\*</sup>, Mark A Walkley<sup>1</sup>

<sup>1</sup>School of Computing, University of Leeds, Leeds, LS2 9JT, UK

<sup>2</sup>School of Mathematical Sciences, Universiti Sains Malaysia, 11800 USM Penang, Malaysia

<sup>3</sup>School of Mathematics, University of Leeds, Leeds, LS2 9JT, UK

Corresponding author, Oliver G Harlen, School of Mathematics, University of Leeds, Leeds, LS2 9JT, UK, email [o.g.harlen@leeds.ac.uk](mailto:o.g.harlen@leeds.ac.uk)

## Abstract

The flow of a bi-disperse polymer melt through a hyperbolic contraction is simulated using the recently proposed Rolie-Double-Poly constitutive model (Boudara *et al*, J. Rheol. **63**,71 (2019)). This simplified tube model takes account of the nonlinear coupling between the dynamics of the long and short-chains in a bi-disperse blend, in particular it reproduces the enhancement of the stretch relaxation time that arises from the coupling between constraint release and chain retraction. Flow calculations are performed by implementing both the Rolie-Double-Poly and multimode Rolie-Poly models in OpenFOAM® using the RheolTool library. While both models predict very similar flow patterns, the enhanced stretch relaxation of the Rolie-Double-Poly models results in an increase in the molecular stretch of the long chain component in the pure extensional flow along the centre-line of the contraction, but a decrease in the stretch in shear-flow near the channel walls.

## Introduction

A key challenge in modelling the flow of polymeric fluids is to develop approximate models that capture the key aspects of the molecular scale dynamics in a form that is amenable for use in computational fluid dynamics. In particular, accurate prediction of flow requires the ability to predict the stresses induced by the flow gradient history experienced by the polymer molecules. However, as well as being able to predict the flow field during processing, the conformation changes produced during processing have a critical effect on both the residual stresses and, in the case of semi-crystalline polymer, the crystalline morphology in the final product.

In recent years considerable progress has been made in developing models for monodisperse linear polymer melts based on the tube theory concept of de Gennes (1971) and Doi and Edwards (1986). Sophisticated constitutive models, such as the GLaMM model (Graham et al 2003) are able to give quantitatively accurate predictions for the behaviour of near monodisperse melts in strongly nonlinear flows (Auhl *et al* 2008). Moreover a simplified version of this model, the RoliePoly (RP) model (Likhtman & Graham 2003) retains the main features of the GLaMM model in form that is amenable for computational fluid dynamics (Collis et al 2005, Lord et al 2010).

However, while these models work well for monodisperse polymer melts, they do not capture the behaviour of blends of polymers of different molecular weights typical of industrial grade polymers. In particular the approach of summing contributions from different modes ignores the effects of interactions between components of different molecular weights. Recently, Boudara et al (2019) have combined ideas from double reptation (des Cloizeaux 1988), that provides a method for capturing interactions between chains of different lengths in linear rheology, with the Rolie-Poly model to provide an approximate model for the nonlinear rheology of polydisperse blends. In this model, named the Rolie -Double-Poly (RDP) model,

the stress contribution from each polymer species is constructed from a sum of contributions from entanglements with each of the other species in the melt. The stress in the blend of  $N$  different components is therefore formed from the sum of  $N^2$  contributions. In their paper Boudara *et al* only consider the behaviour of this model in uniform extensional flow. In this paper we will assess the behaviour in a more complex flow geometry that involves a mixture of shear and extensional flow.

Contraction flows have been widely studied as a prototypical processing geometry containing regions of both shear and extensional flow. The sudden four-to-one contraction was established as a benchmark flow for viscoelastic flow computations and so has been extensively studied both numerically and experimentally. However, here we consider a contraction with a hyperbolic geometry, which in theory, provides a region of approximately uniform extensional flow along the centre-line.

In the following section we set out the RP and RDP constitutive models and describe how we have implemented these in the OpenFOAM® open source CFD toolbox (Weller *et al* 1998) using the RheolTool library (Pimenta & Alves 2017). We then compare the predictions of these models for a bimodal blend flowing through a hyperbolic contraction. In particular we examine the differences in the predictions for the chain-stretch of the high molecular weight component between the RDP and RP models.

### **The Rolie-Poly and Rolie-Double-Poly Constitutive Models**

The original Rolie-Poly (RP) model was proposed by Likhtman and Graham as a highly simplified single-mode approximation to their full chain molecular theory for entangled monodisperse linear polymer chains. The stress  $\sigma$  is obtained from a conformation tensor  $A$  as,

$$\boldsymbol{\sigma} = G\mathbf{A}, \quad (1)$$

where  $G$  is the elastic modulus and  $\mathbf{A}$  evolves as,

$$\overset{\nabla}{\mathbf{A}} = -\frac{1}{\tau_d}(\mathbf{A} - \mathbf{I}) - \frac{2}{\tau_s}(1 - \lambda^{-1})\mathbf{A} - \frac{\beta_{th}}{\tau_d}(\mathbf{A} - \mathbf{I}) - \frac{2\beta_{CCR}\lambda^{2\delta}}{\tau_s}(1 - \lambda^{-1})(\mathbf{A} - \mathbf{I}). \quad (2)$$

The left-hand side is the upper-convected time derivative of  $\mathbf{A}$  and the four terms on the right-hand side represent respectively relaxation from: reptation; chain retraction; thermal constraint release and convective constraint release. Here,  $\lambda = \sqrt{\text{Tr}\mathbf{A}/3}$  represents the ratio of the tube-length of the polymer to its equilibrium value, which relaxes on the tube Rouse time,  $\tau_s$  whereas the orientation of  $\mathbf{A}$  relaxes on the tube reptation time,  $\tau_d$ . The parameters  $\beta_{th}$ ,  $\beta_{CCR}$  and  $\delta$  control the rates of thermal and convective constraint release. In the multimode Rolie-Poly model the stress is computed as the sum of contributions from the different modes,

$$\boldsymbol{\sigma} = \sum G_i \mathbf{A}_i. \quad (3)$$

In the Rolie-Double-Poly model (Boudara *et al* 2019) the stress remains given by the sum of contributions from different species, but each in turn contains separate contributions from entanglements with each of the other species in the blend. For ease of presentation we will just consider the case of a bi-disperse blend consisting of long and short chains labelled  $L$  and  $S$  respectively, of volume fractions  $\varphi_L$  and  $\varphi_S$ . Note that Boudara *et al* (2019) include the effects of finite extensibility, which we have neglected. We assume that blend is made of two different molecular weights of the same polymer so that elastic moduli are proportional to  $\varphi_L$  and  $\varphi_S$ , so that the stress is given by

$$\boldsymbol{\sigma} = G(\varphi_L \mathbf{A}_L + \varphi_S \mathbf{A}_S), \quad (4)$$

where  $\mathbf{A}_L$  and  $\mathbf{A}_S$  are the conformation tensors for the long and short chains with stretches given by  $\lambda_L = \sqrt{\text{Tr}\mathbf{A}_L/3}$  and  $\lambda_S = \sqrt{\text{Tr}\mathbf{A}_S/3}$  respectively. However, each of  $\mathbf{A}_L$  and  $\mathbf{A}_S$  are now written as sum of contributions from interactions with the long and short chains as

$$\mathbf{A}_L = \varphi_L \mathbf{A}_{LL} + \varphi_S \mathbf{A}_{LS}, \quad (5a)$$

$$\mathbf{A}_S = \varphi_L \mathbf{A}_{SL} + \varphi_S \mathbf{A}_{SS}, \quad (5b)$$

where  $\mathbf{A}_{IJ}$  denotes the contributions to the conformation of chains of type  $I$  from entanglements with chains of type  $J$ . Each tensor  $\mathbf{A}_{IJ}$  satisfies an evolution equation of the form,

$$\nabla \mathbf{A}_{IJ} = -\frac{1}{\tau_{d,I}} (\mathbf{A}_{IJ} - \mathbf{I}) - \frac{2}{\tau_{s,I}} (1 - \lambda_I^{-1}) \mathbf{A}_{IJ} - \frac{\beta_{th}}{\tau_{d,J}} (\mathbf{A}_{IJ} - \mathbf{I}) - \frac{2\beta_{CCR} \lambda_J^{2\delta}}{\tau_{s,J}} (1 - \lambda_J^{-1}) (\mathbf{A}_{IJ} - \mathbf{I}). \quad (6)$$

The differences from the RP model is that while the reptation and retraction rates are governed by the reptation and Rouse relaxation times (and stretch) of the  $I$  chains, the constraint release terms are determined by the properties of the “tube” created by the  $J$  chains.

To compare the behaviour of this model with that of a multimode RP model we shall consider a bimodal blend consisting of  $S$ -chains with  $\tau_{d,S} = 0.1$ ,  $\tau_{s,S} = 0.05$  in arbitrary units blended with  $\varphi_L = 0.05$  of  $L$ -chains  $\tau_{d,L} = 10$ ,  $\tau_{s,L} = 1$ . Here  $\beta_{th} = 1$  and  $\beta_{CCR} = 0$ . This could be compared to a two mode RP model where the relaxation times are taken to be those of the  $L$  and  $S$  components. However such a model does not even give the same linear rheology as the RDP model, whereas the common practice in constructing a multimode RP spectrum is to assign the reptation/orientation relaxation times and moduli to fit to the measured linear rheology. Hence we shall compare to a three mode RP model with

$$\tau_{d,1} = \frac{\tau_{d,L}}{2}, \quad \tau_{d,2} = \left( \frac{1}{\tau_{d,L}} + \frac{1}{\tau_{d,S}} \right)^{-1}, \quad \tau_{d,3} = \frac{\tau_{d,S}}{2}, \quad (7a)$$

$$G_1 = G\phi_L^2, \quad G_2 = 2G\phi_L\phi_S, \quad G_3 = G\phi_S^2, \quad (7b)$$

so that the two models give the same predictions in the linear viscoelastic limit. Note that in the limit  $\tau_{d,L} \gg \tau_{d,S}$ ,  $\tau_{d,2} \approx \tau_{d,S}$ . Hence we can think of the first mode as representing the *LL* conformation, the second as the *LS* and *SL* conformations and the third as the *SS*

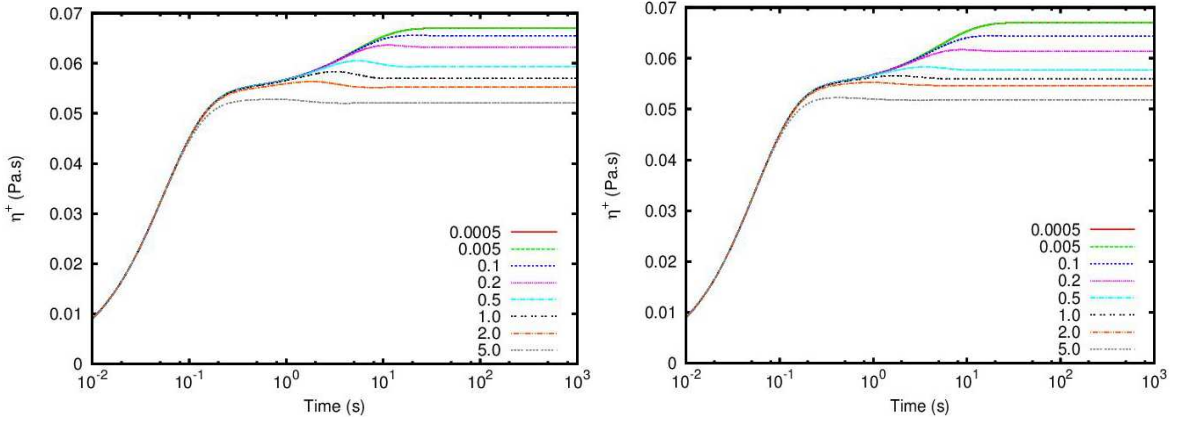


Figure 1: Comparison of the transient shear viscosity,  $\sigma_{xy}/\dot{\gamma}$ , between the RDP (left) and 3 mode RP (right) models at a range of different shear-rates. The predictions of the two models are nearly identical.

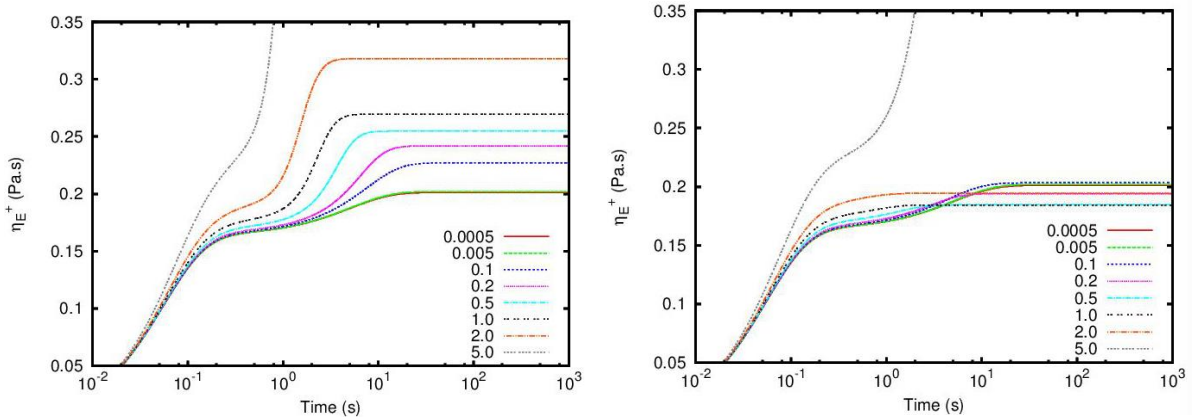


Figure 2: Comparison of the transient extensional viscosity between the RDP (left) and 3

mode RP models (right) at different extension-rates. The RDP strain hardens at extension rates below  $1/\tau_{s,L}$  due to enhanced stretch relaxation.

conformation. Although not set by linear viscoelasticity, we assign the stretch relaxation times in a similar way as,

$$\tau_{s,1} = \tau_{s,L}, \quad \tau_{s,2} = 2 \left( \frac{1}{\tau_{s,L}} + \frac{1}{\tau_{s,S}} \right)^{-1}, \quad \tau_{s,3} = \tau_{s,S}. \quad (7c)$$

Comparing figure 1 and 2, we observe that while the predictions of these two models in shear flow are very similar, there is a marked difference in the behaviour in extensional flow. In particular the RDP model exhibits strain-hardening at extension rates below  $1/\tau_{s,L}$  due to the phenomenon of enhanced stretch relaxation (Read *et al* 2012) of the long chain component in a bi-disperse blend. This increases the effective stretch relaxation time of the long chains within the constraint tube composed of the other long chains to  $\tau_{s,L}/\phi_L$  (see Read *et al* 2012, Boudara *et al* 2019).

### **OpenFOAM Simulations**

To compare the predictions of these models in more complex flow geometries requires implementing these models within a computational fluid dynamics solver. Here we use OpenFOAM®, which is an open-source finite-volume solver for solving partial differential equations on unstructured meshes in two and three-dimensions. In particular, a number of different general viscoelastic solvers have been developed in OpenFOAM®. Here we use the rheoTool solver (Pimenta & Alves 2017). This uses the SIMPLEC algorithm for the pressure-velocity coupling and the CUBISTA scheme to discretize the convection terms, resulting in an algorithm that is second-order accurate in both time and space.

The stability and accuracy of the RheoTool library for the flow of an Oldroyd-B fluid through a sudden 4:1 contraction are discussed by Pimenta & Alves (2017), who found good agreement with previous calculations including their in-house finite volume code for Deborah numbers up to 12.

We have modified the rheoTool solver by adding functions for both the multimode RoliePoly (mRP) and Rolie-Double-Poly (RDP) models. The implementation of the mRP was verified through comparison with the mRP contraction flow simulations of Tenchev et al (2011). Furthermore, the implementation of the RDP model has been validated against transient uniaxial extension calculations given by Boudara *et al* (2019).

### Hyperbolic Contraction Flow

Although the sudden contraction flow is a popular choice for a flow with an extensional component, the strain-rate history through the contraction is complex and depends strongly upon the rheological properties of the fluid (as this affects the flow pattern upstream of the contraction). However, if instead the shape of the contraction is chosen to be hyperbolic then in the case of perfect slip at the walls the polymer will experience a constant rate of extension through the contraction and so has been used to measure extensional properties (James *et al* 1990, Collier *et al* 1998) of polymeric fluids.

In this paper we shall consider a planar hyperbolic contraction flow within a channel with centre-line along the  $x$  axis, where the half-height  $H(x)$  is defined as,

$$H(x) = \begin{cases} H_0, & x \leq 0, \\ \frac{H_0 L}{L + (H_0/H_1 - 1)x}, & 0 < x < L, \\ H_1, & x \geq L, \end{cases} \quad (8)$$

so that the channel-half height contracts from  $H_0$  to  $H_1$  over a length  $L$ . Our numerical experiments with different geometries show that provided  $2 H_0/L \leq 1$  there is a region of

approximately uniform extension-rate along the centre-line,  $y = 0$ , for  $0 \leq x \leq L$ . We shall therefore consider two different contractions: a 4:1 contraction with  $H_0 = 1$ ,  $H_1 = 0.25$  and  $L = 5$  and a 10:1 contraction with  $H_0 = 2.5$ .

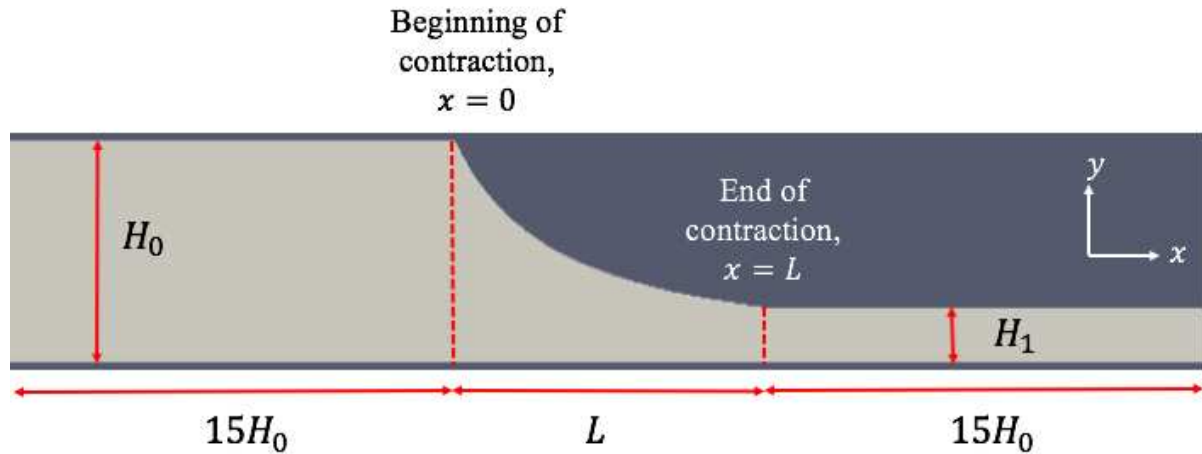


Figure 3: The computational domain for the planar hyperbolic contraction flow.

The computational domain is shown in figure 3. As the flow is symmetric about the centre-line only half the domain is calculated. The flow through the contraction is driven by imposing the pressure difference between the inlet and outlet. At the walls a no-slip boundary condition is applied to the velocity, whilst linear extrapolation (Pimenta & Alves 2017) is used to provide a boundary condition for the conformation tensors at the wall. The steady state solution was obtained from a transient calculation in which the upstream pressure was initially increased as,  $P = \alpha(1 - e^{-\beta t})$  in order to give a smooth onset. The form of this pressure ramp had no effect on the final steady state.

The finite volume solution uses the default schemes from the rheoTool package with the SIMPLEC algorithm used for the pressure-velocity coupling and CUBSITA used to discretise the convective terms. A preconditioned Bi-Conjugate Gradient solver with an incomplete LU preconditioner was used to solve the pressure equation with a relative tolerance of  $10^{-7}$ .

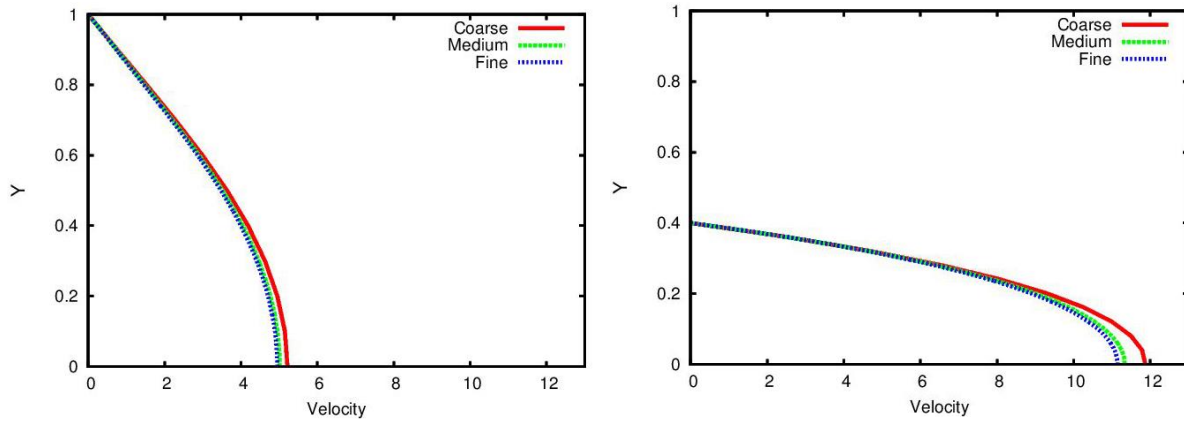


Figure 4: The velocity profile across the geometry predicted using different mesh resolution. The mesh refinement is made by increasing the number of cell by factor 2 and 4 in both  $x$  and  $y$  direction from coarse to medium and from coarse to fine respectively. Left-hand side figure (a) is taken at  $x = -0.2$  (upstream). Right-hand side figure (b) is taken at  $x = 2.5$  (mid-way of contraction).

Three different meshes were used for the 4:1 hyperbolic contraction flow, all formed from a single block of quadrilateral elements, denoted coarse (210 cells in  $x$  direction and 10 cells in  $y$  direction), medium (410 x 20) and fine (840 x 40). Figure 4 shows the convergence of the velocity in the upstream and downstream channel for these different meshes. Due to the higher contraction ratio the mesh for the 10:1 contraction was constructed from multiple blocks to avoid elements with a high skewness and consisted of 7500 elements.

Figure 5 compares the fluid velocity along the centre-line and the corresponding centre-line extension rate for these two contraction geometries for the RDP model, where we have chosen the flow rates such that the extension rates are approximately equal. However, since the flow-rate in the 10:1 contraction is lower, the melt has a longer residence time in the contraction and therefore experiences a higher strain.

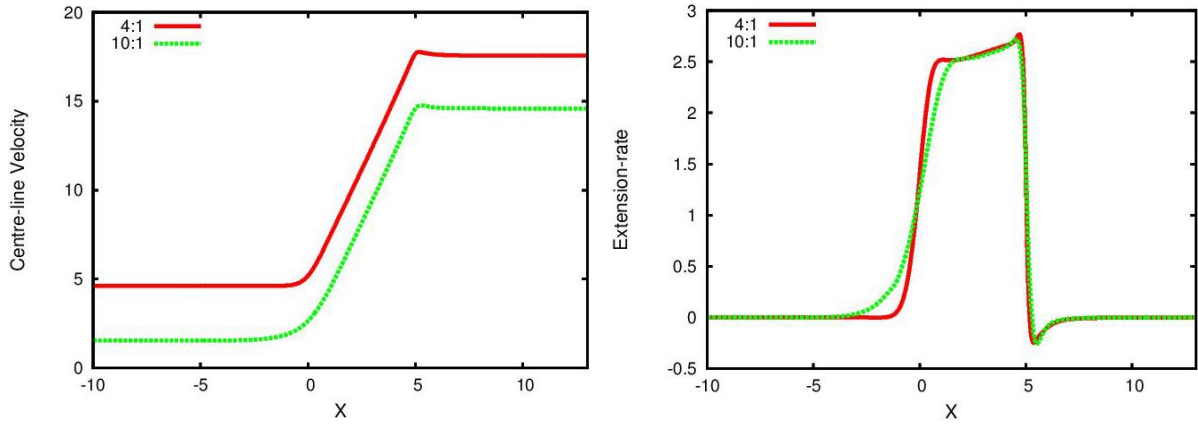


Figure 5: Comparison of the velocity and extension rate along the centre-line between the 4:1 and 10:1 hyperbolic contractions for the RDP model. Both geometries give an approximately linear increase in velocity within the contraction region  $0 \leq x \leq 5$ . The ratio of the flow-rates between the two geometries have been chosen to give approximately the same extension rate.

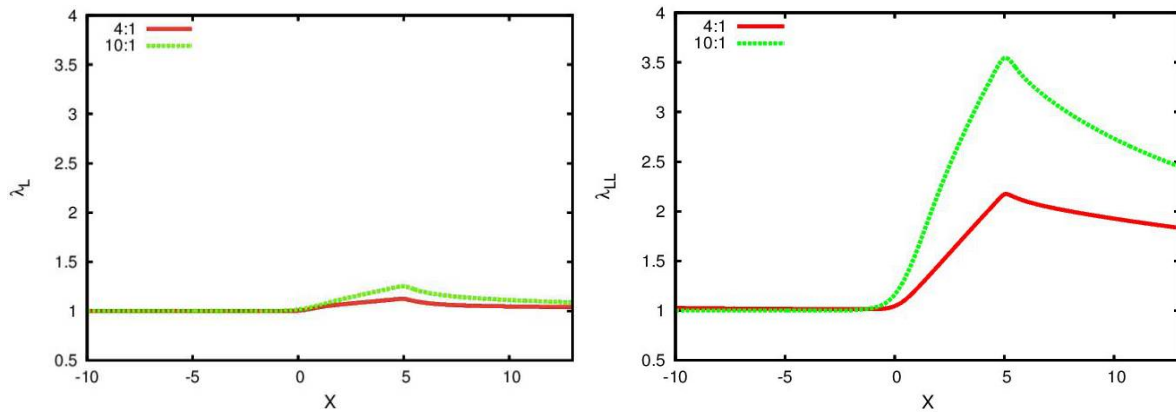


Figure 6: Graphs showing the extension of the  $L$ -chain component along the centre-line of the 4:1 and 10:1 hyperbolic contractions for the RDP model. Left-hand figure (a) shows the stretch  $\lambda_L = \sqrt{\text{Tr}\mathbf{A}_L/3}$  in the “thin tube” formed from both  $L$  and  $S$  chains. Right-hand figure (b) shows the stretch in the “fat tube” composed only of  $L$ - chains,  $\lambda_{LL} = \sqrt{\text{Tr}\mathbf{A}_{LL}/3}$ .

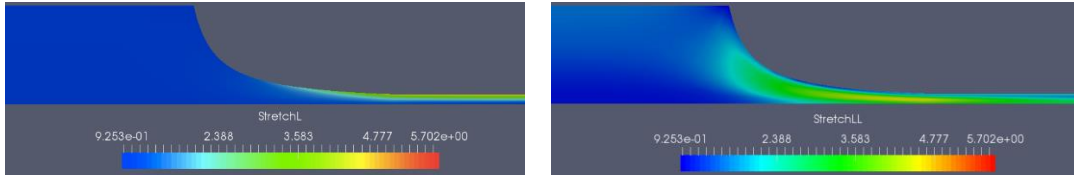


Figure 7: Colour maps showing the extension of the  $L$ -chain component in the 10:1 hyperbolic contraction for the RDP model. Left-hand figure (a) shows the stretch  $\lambda_L = \sqrt{\text{Tr}\mathbf{A}_L/3}$  in the “thin tube” formed from both  $L$  and  $S$  chains. Right-hand figure (b) shows the stretch in the “fat tube” composed only of  $L$ - chains,  $\lambda_{LL} = \sqrt{\text{Tr}\mathbf{A}_{LL}/3}$ .

### Chain Stretch in the Hyperbolic Contraction Flow

From figure 5 we observe that the maximum extension rate,  $\dot{\epsilon}$  along the centre line is around 2.5, meaning that  $\dot{\epsilon}\tau_{s,L}$  is less than unity. This means we would not expect to find significant chain stretching in a melt consisting entirely of  $L$ -chains. However, for a 5% blend the effective stretch relaxation time is enhanced by a factor of 20, giving  $\dot{\epsilon}\tau_{s,L}/\varphi_L = 10$  so we might expect to see some stretching of the long chains in a blend. Figure 6a shows the stretch,  $\lambda_L$  along the centre-line of the 4:1 and 10:1 contractions, but shows only a very slight stretch as the melt flows through the contraction. However,  $\lambda_L$  represents the chain-stretch with respect to the tube generated by all the chains in the melt and since  $L$ -chains make up only 5%, it is dominated by the short-lived entanglements with the  $S$ -chains. If we instead examine the stretch within the tube composed only of  $L$ - chains, (sometimes referred to as the “fat-tube”),  $\lambda_{LL} = \sqrt{\text{Tr}\mathbf{A}_{LL}/3}$ , shown in figure 6b, then we do indeed see a significant increase in stretch from the effects of enhanced stretch relaxation.

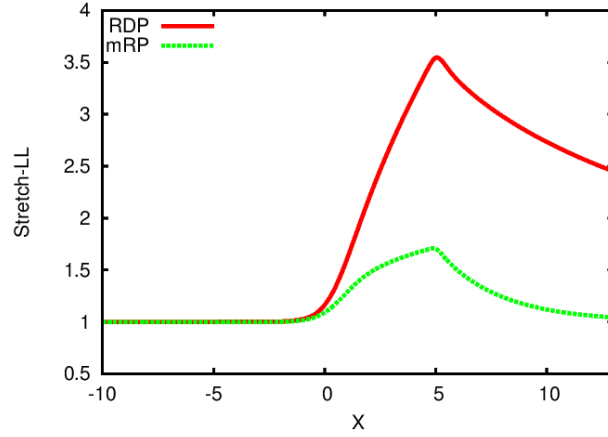


Figure 8: Graph comparing the centre-line values of  $\lambda_{LL} = \sqrt{\text{Tr}\mathbf{A}_{LL}/3}$  for the RDP model with stretch of the first mode in the multimode RP model.

Although the extension rate in the contraction is around 2.5, the shear-rate at the wall downstream of the contraction is around 140, more than a factor of 50 larger than the extension rate. Consequently, although the flow along the centre-line is extensional, away from the centre-line the velocity gradient is dominated by shear. Figure 7 shows the values of  $\lambda_L$  and  $\lambda_{LL}$  in the 10:1 contraction. The highest values of  $\lambda_L$  are found in the regions of highest shear-rate next to the wall downstream of the contraction. The distribution of  $\lambda_{LL}$  is quite different. Although the stretch initially increases as we move away from the axis, it then decreases as we approach the wall. In shear-flow the chains tend to align away from the velocity gradient and stretch of the  $L$ -chains comes as a result of constraint release from short-chains that relaxes the orientation.

Finally, in figure 8, we compare the stretch of the first mode in the mRP model with  $\lambda_{LL}$  along the centre-line of the 10:1 contraction. Although the first mode of the Rolie-Poly spectrum represents the  $LL$  entanglements it doesn't include the enhancement of the stretch relaxation time and so gives a much lower prediction for the stretch, as predicted from the extensional rheology shown in figure 2. Moreover, the stretch that is produced decays quickly with downstream distance whereas the stretch in RDP model persists well beyond the contraction.

## **Conclusions**

The Rolie-Double-Poly model provides a simplified constitutive model for polymer blends that incorporates the effects of the coupling between different components on the nonlinear rheology. In this paper we have shown that this model is sufficiently simple to be used for computational fluid dynamics calculations in complex geometries. We also find that the predictions for stretch of the long chain component are markedly different from that of a multimode Rolie-Poly model with the same linear rheology.

Although we have only shown results for two-dimensional calculations here, the extension to a fully three-dimensional flow is straight-forward. More challenging is to extend the model to a fully polydisperse blend made up of  $N$  components, requiring  $N^2$  modes to be calculated.

The geometric constraints of the contraction flow studied mean that the flow pattern of the two models is very similar. However, conformation changes produced during processing can critically affect the final product. For example, in a semi-crystalline polymer chain stretch can dramatically increase the rate of crystal nucleation by reducing the entropic penalty for crystallisation.

## **Acknowledgements**

AA would like to acknowledge funding from the Ministry of Education Malaysia and the Universiti Sains Malaysia. OGH also acknowledges funding from EPSRC Grant Ref. EP/P005403/1.

We would like to thank Victor Boudara and Daniel Read for helpful insights and discussions on the Rolie-Double-Poly model.

## References

- Auhl, D., J. Ramirez, A. E. Likhtman, P. Chambon, and C. Fernyhough, 2008, Linear and nonlinear shear flow behavior of monodisperse polyisoprene melts with a large range of molecular weights, *J. Rheol.* **52**, 801–835.
- Boudara V.A.H., D.J. Read, J.D. Peterson, L.G. Leal, 2018, Nonlinear rheology of polydisperse blends of entangled linear polymers: Rolie-Double-Poly models, *J. Rheol.* **63**, 71-91.
- Collier J.R. O. Romansoschi, and S. Petrovan, 1998, Elongational Rheology of Polymer Melts and Solutions, *J. App. Poly. Sci.* **69**, 2357-2367.
- Collis, M. W., A. K. Lele, M. R. Mackley, R. S. Graham, D. J. Groves, A. E. Likhtman, T. M. Nicholson, O. G. Harlen, T. C. B. McLeish, L. R. Hutchings, C. M. Fernyhough, and R. N. Young, 2005, Constriction flows of monodisperse linear entangled polymers: Multiscale modelling and flow visualization, *J. Rheol.* **49**, 501–522.
- de Gennes, P.-G., 1971, Reptation of a polymer chain in the presence of fixed obstacles, *J. Chem. Phys.* **55**, 572–579.
- des Cloizeaux, J., 1988, Double reptation vs. Simple reptation in polymer melts, *Europhys. Lett.* **5**, 437–442.
- Doi, M., and S. F. Edwards, 1986, *The Theory of Polymer Dynamics*, Oxford University Press.
- Fattal, R., and R. Kupferman, 2004, Constitutive laws for the matrix-logarithm of the conformation tensor. *J. Non-Newton. Fluid Mech.* **123**, 281-285.

Graham, R. S., A. E. Likhtman, T. C. B. McLeish, and S. T. Milner, 2003 “Microscopic theory of linear, entangled polymer chains under rapid deformation including chain stretch and convective constraint release, *J. Rheol.* **47**, 1171–1200.

James, D.F., G.M. Chandler, S.J. Armour 1990, A converging channel rheometer for the measurement of extensional viscosity, *J. Non-Newton. Fluid Mech.* **166**, 307-320.

Likhtman, A. E., and R. S. Graham, 2003 “Simple constitutive equation for linear polymer melts derived from molecular theory: Rolie-Poly equation,” *J. Non-Newton. Fluid Mech.* **114**, 1–12.

Lord, T. D., L. Scelsi, D. G. Hassell, M. R. Mackley, J. Embery, D. Auhl, O. G. Harlen, R. Tenchev, P. K. Jimack, and M. A. Walkley, 2010, The matching of 3D Rolie-Poly viscoelastic numerical simulations with experimental polymer melt flow within a slit and a cross-slot geometry,” *J. Rheol.* **54**, 355–373.

Pimenta F., M.A. Alves 2017, Stabilization of an open-source finite-volume solver for viscoelastic fluid flows, *J. Non-Newton. Fluid Mech.* **239**, 85-104.

Read, D. J., K. Jagannathan, S. K. Sukumaran, and D. Auhl, 2012, A full-chain constitutive model for bidisperse blends of linear polymers, *J. Rheol.* **56**, 823–873.

Tenchev R., T. Gough, O.G. Harlen, P.K. Jimack, D.H. Klein and M.A. Walkley 2011, Three-dimensional finite element analysis of the flow of polymer melts, *J. Non-Newton. Fluid Mech.* **166**, 307-320.

Weller H.G., G. Tabor, H. Jasak and C. Fureby 1998, A tensorial approach to computational continuum mechanics using object orientated techniques, *Comput. Phys.*, **12**, 620-631.